

Supplemental data

Methods

Cell culture

Primary macrophages were isolated from murine bone marrow cells and cultured as previously described¹ in Dulbecco's modified Eagle medium (DMEM, Sigma, Israel) supplemented with 30% L929-conditioned medium, 20% fetal bovine serum (FBS), 2mM L-glutamine, 100 units/mL Penicillin and 100 µg/mL Streptomycin (All from Biological Industries, Israel). After six days of proliferation and differentiation, cells were washed, detached with PBS containing 0.02% EDTA (Sigma), centrifuged and re-suspended in DMEM supplemented with 10% FBS, 2mM L-glutamine, 100 units/mL Penicillin and 100 µg/mL Streptomycin (All from Biological Industries). RAW264.7 macrophages were grown in DMEM supplemented with 10% heat-inactivated FBS, 2mM L-glutamine, 100 units/mL Penicillin and 100 µg/mL Streptomycin. All cells were incubated in an atmosphere of 37°C, 5% CO₂ and 95% humidity.

Animal studies

For ferrozine iron assay and blood tests, 12 weeks old male mice were euthanized by injection of sodium pentobarbital and dipped in 70% ethanol for 5 min. The thoracic cavity was opened. The heard blood with or without anticoagulant (EDTA) was collected and centrifuged at 4000 x g for 10 min. The supernatant plasma or serum was collected. The plasma served for complete blood count (CBC) test while the serum served for serum iron and total iron-binding capacity (TIBC) test. Company names used: Beijing North Biotechnology Research Institute and Zhejiang DIAN Diagnostics Co., Ltd. (both in China).

Mutant mice

BLOC-1 is composed of proteins encoded by the *pallid*, *muted*, *sandy* (*HPS7*), *cappuccino* and *reduced pigmentation* (*HPS8*) HPS genes together with three additional novel subunits. BLOC-2 is composed of proteins encoded by the *cocoa* (*HPS3*), *ruby-eye 2* (*HPS5*) and *ruby-eye* (*HPS6*) genes. BLOC-3 contains proteins encoded by the *pale ear* (*HPS1*) and *light ear* (*HPS4*) genes. BLOC1^{-/-} mice (*pa* strain) tested in this research have a nonsense mutation in the *pallid* gene which causes a truncated Pallidin protein (undetectable by Western blot) and affects the stability of other subunits of the BLOC-1 complex.^{2,3} BLOC2^{-/-} mice (*ru* strain) have an in-frame deletion mutation in the *ruby-eye* gene which disrupts the function of the Hps-6 protein.⁴ BLOC3^{-/-} mice (*ep* strain) have an in-frame insertion mutation in the *pale ear* gene and is associated with a large genomic alteration and defective Hps-1 protein function.⁵⁻⁷ Rab27A^{-/-} (*ash* strain) mice have a splicing mutation in the *RAB27A* gene which results in protein-null mutation.⁸⁻¹⁰ All mice are viable and healthy and the most visually apparent effects are on pigmentation of the coat and eyes.¹¹⁻¹⁴

Immunofluorescence

Immunofluorescence staining was performed as previously described.^{15,16} Briefly, macrophages were grown on sterile coverslips (13mm, Thermo Fisher Scientific, MS, U.S.A) in 24-well cell culture plate at approximately 300 x 10⁵ cells/well and were treated with agents as indicated. Then, cells were washed, fixed with 4% PFA in PBS (Electron Microscopy Sciences, PA, U.S.A), permeabilized with 0.1% Triton X-100, blocked with 10% normal serum in 0.1% BSA (Biological Industries) and incubated with primary antibodies. Affinity purified rabbit anti-L-ferritin (a kind gift from Prof. A.M. Konijn, Hebrew University of Jerusalem,

Israel, 1:400), rat anti-GM-130 (BD Bioscience, 1:200), goat anti-EEA-1 (Santa Cruz, 1:200) and goat anti-CatD (R&D Systems, 1:200) antibodies were incubated over-night (ON) in 0.1% BSA at room temperature (RT). Next, cells were washed, incubated with secondary antibodies (Alexa Fluor, ThermoFisher Scientific, MA, USA) for 1 h, washed and mounted with DAPI (Vector Laboratories, Inc. CA, U.S.A). Negative controls were done to exclude non-specific staining and channel leakage.

Ferrozine iron assays

Liver iron content was measured using a colorimetric ferrozine-based assay¹⁷ with some modifications. Briefly, 22 μ l concentrated HCl (11.6 mol/L) was added to 100 μ l cell lysate (~500 μ g total protein). The mixed sample was heated at 95°C for 20 min, then centrifuged at 12,000 \times g for 10 min. Supernatant was transferred very gently into fresh tubes. Ascorbate was added to reduce the Fe (III) into Fe (II). After 2 min of incubation at RT, ferrozine and saturate ammonium acetate (NH₄Ac) were sequentially added to each tube and the absorbance was measured at 570 nm (BioTek EL x 800, Shanghai, China) within 30 min.

Subcellular fractionation

Cells were lysed in ice-cold lysis buffer containing 1% Triton X-100, 20mM Tris, 37mM NaCl, 10% Glycerol, 10 μ g/mL leupeptin and a tablet of EDTA-free protease inhibitor cocktail (Roche Diagnostic, Mannheim, Germany)/10 mL lysis buffer. The lysates were incubated on ice, centrifuged at 10,000 \times g for 10 min at 4°C and supernatants were collected. Differential detergent fractionation was performed as previously described¹⁸ with minor modifications. Cell suspensions were pelleted and washed by centrifugation at 200 \times g and 4°C. Next, cells were washed with Reduced H medium+ protease inhibitors (RHM+) buffer containing 210 mM mannitol, 70 mM sucrose, 4 mM HEPES pH 7.2, 1 mM AEBSF and one protease inhibitor tablet/10 mL buffer. Cell pellets were re-suspended in RHM+ buffer containing 0.2% digitonin and incubated on ice. Cell lysates were centrifuged at 700 \times g and the supernatants were centrifuged at 16,000 \times g. The final supernatants were considered as the cytosolic fraction. The pellets after the 700 \times g centrifugation step were washed with RHM+ buffer at 16,000 \times g, lysed with 1% Triton X-100 lysis buffer and centrifuged again. This was considered the membrane-bound vesicles fraction. Subcellular fractionation for lysosome-enriched fractions was performed as previously described.¹⁹

Immunoblotting analysis

Samples were separated by SDS-PAGE and transferred to nitrocellulose. Blots were incubated with antibodies diluted in blocking buffer for 1 hr. Anti-L-ferritin and H-ferritin (kind gifts from Prof. A.M. Konijn, 1:5,000) was incubated for 1 h in 3% BSA in TBS-T buffer at RT. Anti-LAMP1 (Abcam, Cambridge, UK, 1:5,000), anti-Tubulin (kind gift from Prop. Gera Neufeld, 1:1000), Anti-TSG101 (Abcam, 1:500), anti-TNF α (Santa Cruz Biotechnology, Inc. Dallas, Texas, U.S.A), anti-TfR1 (Invitrogen, CA, U.S.A) and anti- β -actin (Bioworld technology, Inc. MN, U.S.A) antibodies were used according to the manufacturer's recommendations. The membrane was washed with TBS-T buffer, incubated with horseradish peroxidase-conjugated secondary antibodies (Abcam, 1:25,000) and detected with enhanced chemiluminescence kit (Thermo Fisher Scientific, MA, USA).

Isolation of exosomes by ultracentrifugation

Exosomes were isolated from cell culture medium as previously described.²⁰ At least three confluent 10 cm² plates of cells were washed twice and incubated at 37°C in 1:1 mixture of OptiMEM I medium (Gibco by Life Technologies, Thermo Fisher Scientific, MA, USA) and complete DMEM medium supplemented with 1mg/L

BSA, 20mM β -mercaptoethanol and 100 μ M FAC. After 24 h, medium was collected and placed on ice, and the cells were lysed in 1% Triton X-100 lysis buffer. The medium was then centrifuged for 10 min at 2,000 x *g* and 4°C to remove dead cells and for 30 min at 12,000 x *g* and 4°C to remove cell debris using Optima L-90K ultracentrifuge with fixed Type 70 Ti rotor (Beckman Coulter, Inc. CA, U.S.A). The supernatant was collected and centrifuged for 90 min at 100,000 x *g* and 4°C to sediment the exosomal fraction. The pellet was washed and centrifuged for additional 90 min at 100,000 x *g* and 4°C to remove soluble serum and contaminating secreted proteins. Additional washes were performed. Finally, the pellet containing the exosomes was re-suspended in ice-cold PBS and the sample was resolved by SDS-PAGE and analyzed by immunoblotting. Alternatively, exosomal fractions were analyzed by TEM analysis.

Transmission electron microscopy (TEM) analysis

Ferritin cores were determined by TEM using a JEOL (JEM-2100) Electron Microscope operated at 200 KeV from the Centro Nacional de Microscopía Electrónica (CNME), Spain. Samples were diluted in water and a drop of the suspension was mounted on a carbon-coated copper grid, allowing the water to evaporate slowly at RT. Images were routinely taken at 40kx and 100kx magnifications using a Gatan Orius SC1000 (Model 832) CCD. Iron analysis was performed by Energy Dispersive Spectroscopy (EDS) (OXFORD INCA). Negative staining and cryo-TEM experiments were done at the Technion - IIT. For negative staining, samples were supplemented with 0.1% glutaraldehyde. A 400-mesh carbon-coated grid was placed on a 20 μ l sample drop and blotted with a filter paper. The samples were chemically stained by placing the grid on a 20 μ l drop of 1% uranyl acetate followed by blotting with a filter paper and air-drying. Talos F200C and Tecnai T12 G2 TEMs (FEI, Netherlands) were used for analysis. Images were recorded digitally on Ceta (FEI, Netherlands) or Gatan Ultrascan 1000 camera using the DigitalMicrograph software (Gatan, U.K.). Cryo-TEM samples were prepared under controlled relative humidity and temperature. A 5 μ l drop was placed on a perforated carbon-coated grid. The sample was thinned to ~100-150 nm thick film, quenched in liquid ethane to create a vitrified film and transferred to liquid nitrogen. The vitrified sample was examined in the Tecnai T12 G2 TEM at magnifications of up to 30K under low dose conditions and using imaging procedures as described.²¹

ELISA

Ferritin in murine sera was detected and quantified by sandwich ELISA as described.²² Briefly, a 96-well plate was coated with the goat anti-rat liver ferritin antibody (a kind gift from Prof. A.M. Konijn, 1:5,000) and incubated for 1 h at 37°C and ON at 4°C. Then, the plate was washed and mouse serum samples were diluted and added to the plate. The plate was incubated for 1 h and then washed. Next, the primary antibody rabbit anti-mouse liver ferritin (a kind gift from Prof. A.M. Konijn, 1:10,000) was added, the plate was incubated for 1 h and then washed. The secondary antibody - goat anti-Rabbit IgG beta-galactosidase conjugated human absorbed (Southern Biotech, AL, U.S.A, 1:25,000) was added, the plate was incubated for 1 h and washed. Next, the substrate CPRG (Roche) was added and the plate was incubated for 1.5 h until a chromogenic signal was developed and read in a 96-well plate reader (HR801, Hua Ke Rui, China) at 595 nm. ELISA kits for CRP (Boster, CA, USA) and IL-6 (ExCell Biotech Co., Ltd, Shanghai, China) were according to the manufacturer's recommendations.

Metabolic labeling and pulse-chase analysis

Cells were starved for 30 min at 37°C in L-cysteine/L-methionine-free DMEM (Sigma) supplemented with 10% dialyzed FCS, 0.01M HEPES, 2mM L-glutamine, 100 units/mL Penicillin and 100 μ g/mL Streptomycin. Next, cells were pulse-labeled for 15 min in Figure 4A experiment and for 2 h in Figure 5H experiment, both at 37°C in L-cysteine/L-methionine-free DMEM supplemented with 3mCi \ 15 mL of EasyTag™ EXPRESS³⁵S Protein Labeling Mix, [³⁵S] (Perkin Elmer, MS, U.S.A). Total ³⁵S incorporation was the same in

all samples. The medium was then removed and complete DMEM medium supplemented with 0.5 mg/mL L-cysteine and 0.1 mg/mL L-methionine was added and incubated for the indicated times at 37°C. Cells were washed in ice-cold PBS. When mentioned, all steps, including starvation, pulse-chase labeling and washes, were done in the presence of 100 µM FAC and 5µg/mL brefeldin A (BFA) where indicated. Medium samples were collected at the indicated times and centrifuged. In Figure 5H, cells were not harvested at time 0 h. Cells were lysed in 1% Triton X-100 lysis buffer. For data in Figure 4A, all samples were immunoprecipitated with an anti murine L-ferritin antibody that is specific for the L-subunit, but pulls down the 24-mer. Thus, also H-subunits that are assembled with L-subunits in the whole ferritin multimer. The immunoprecipitate was then separated on SDS-PAGE and the two subunits were separated. Therefore, due to the metabolic labeling we were able to visualize the H-ferritin subunit on the same gel as well, in accordance with results from our previous research²³ in which these two subunits were visualized in a similar manner. In Figure 5H, we used an H-subunit specific antibody for the immunoprecipitation. There, in the HeLa cells with the double deletion of human H- and L-subunit, that were transfected with murine H-subunit only, a single H-subunit band is visible, but in the control RAW264.7 cells, the H-specific antibody also pulled down the L-subunit in the heteropolymer. All gels were run at 50V ON and fixed in 40% (v/v) methanol and 10% (v/v) acetic acid solution, dried and placed in a Kodak screen for S³⁵ according to manufactures instructions and exposed ON to a KODAK BioMax MS film. Radioactive bands were visualized by the Fluorescent image analyzer FLA-7,000 (Typhoon).

Computational tools

Selection of sequences: Based on the availability of Uniprot database,²⁴ ferritin sequences of representative eukaryotic species were selected for surveying signal peptide (SP) presence. The protein sequences of the available eukaryotic species were downloaded and filtered to avoid partial or irrelevant data. Among others, plant-ferritins (also found in the plastids²⁵ and assumed to lack the SP) showed high inconsistency and thus were systematically filtered. To analyze only one single, longest, preferably reviewed sequence per organism, duplications due to multiplicity of variants or subunits, were also subject to filtration. SP search: Determination of the presence or absence of the SP sequence in the chosen ferritin sequences was conducted using SignalP 4.0²⁶ with the D-cutoff value of 0.45. Known information from the literature was used as negative control, while Uniprot annotations were used as positive control. Phylogenetic tree generation: A taxonomy-based phylogenetic tree was generated by phyloT²⁷ and Dendroscope²⁸ tools with only the analyzed organisms present. The organisms were tagged with (+) or (-) for the presence or absence of SP sequence according to the search results. Motif search: The ferritin sequences were divided into two groups: SP positive and SP negative. Motif search in SP negative group was conducted using MEME²⁹ tool on sequences longer than 170 amino acids. The five most abundant motifs were provided to the FIMO²⁹ tool for matches scan in the SP positive group. The objective was to identify those that are common in the SP negative group but non-enriched in the SP positive group. Motif visualization: The motif was colored on the mouse H-ferritin crystal structure from the Protein Data Bank (PDB 3wnw) using the Chimera package.³⁰ All Protein-protein interaction sites on ferritin surfaces were predicted by the Optimal Docking Area (ODA) method,³¹ on the same PDB. ODA methodology is able to predict residues involved in protein-protein interfaces from a single protein structure. This tool is used to analyze the optimal desolvation patch on a protein surface to predict potential binding interface sites.

Targeted deletion of human ferritin H- and L-subunits in HeLa cells by CRISPR/Cas9

CRISPR/Cas9 was used to generate clonal FTH-FTL knockout HeLa cell line. High-quality gRNA sequences were previously used by Mancias and colleagues (Mancias et al., 2015) or designed using the crispr.mit.edu

resource, for FTH and L respectively. Both gRNAs were designed to uniquely target the FTH and FTL gene within the genome. The sequences of the gRNAs used were: FTH1 (exon 1) – GACCATGGACAGGTAAACGT, FTL (exon 1) – GGGACTCACCAGAGAGAGGT. We used an all-in-one expression plasmid for simultaneous gRNA and Cas9 expression (Cong et al., 2013; Ran et al., 2013) under two different promoters: pX330-U6-Chimeric_BB-CBh-hSpCas9 vector (Plasmid #42230, Addgene) co-transfected with 500 ng of empty pTK-Hyg vector (Clontech) harboring hygromycin resistance for the selection for FTH gRNA, while pSpCas9(BB)-2A-Puro (PX459) V2.0 vector (Plasmid #62988, Addgene, harbouring puromycin resistance) for FTL gRNA. Cells were transfected using Lipofectamine3000 according to the manufacturer’s instructions. After 48 hours the complete culture medium was supplemented with 300 µg/mL of hygromycin (Sigma) and 1 µg/mL of puromycin (Thermo Scientific) for the selection of positive clones. We waited approximately 3 days and then the cells were seeded by limiting dilution plating to obtain 1 cell/well on 96- well plates and cultured. Clonal colonies were screened for FTH-FTL protein expression by Western Blotting and targeting was confirmed by sequencing analysis.

Site-directed mutagenesis of murine H-ferritin and cloning

Amino acid substitution in *FTH* gene was generated by the PCR-mediated Overlap Extension method³² using mutagenic and flanking primers (Integrated DNA Technologies, Israel), as detailed in Table 1 (Alanine codons are mark in red). PCR amplifications were performed with Q5 DNA polymerase (New England BioLabs, MA, USA), double-digest of amplicons and pmCherry-N1 vector (following the removal of mCherry) was executed by the restriction enzymes EcoR1 and NotI (New England BioLabs) while the ligation reaction of inserts and vector was performed with T4 DNA ligase (New England BioLabs), according to manufacture instructions. The final constructs, with the specific site-directed mutation in FTH gene, were confirmed by sequencing.

Table 1: Mutagenic and flanking primers designed for PCR-mediated Overlap Extension

	Mutagenic Primers (5'-3')	Flanking Primers (5'-3')
WT (EcoRI site)	-	FAAACGCGAATTCACCATG ACCACCGCGTCTC
WT (NotI site)	-	RACCGCGGCCGCTTAGCTC TCATCACCGTGTCCCAG
R79A	FAGCGAGGTGGC GCAAT CTTCCTGCA	-
R79A	RTGCAGGAAGAT TGCGC CACCTCGCT	-
F81A	FGTGGCCGAATC GCACT GCAGGATATAAA	-
F81A	RTTTATATCCTGCAG TG CGATTCGGCCAC	-
Q83A	FGCCGAATCTTCTG GC AGATATAAAGAAACC	-
Q83A	RGGTTTCTTTATATC TGC CAGGAAGTTCGGC	-

Figures

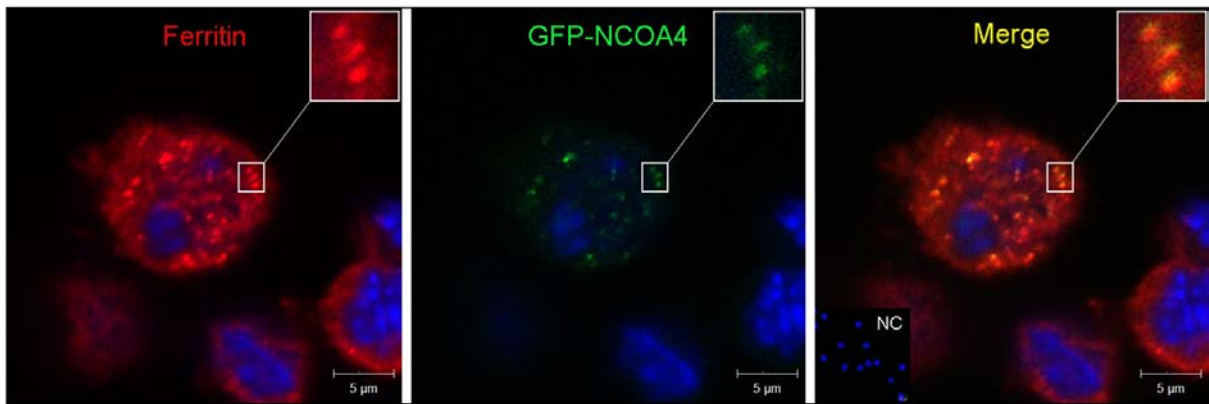


Figure S1. Ferritin co-localizes with NCOA4 - a cargo receptor mediating ferritin transport into the lysosome.³³ Representative confocal images of murine macrophages transfected with GFP-NCOA4 (green) by Lipofectamine 2000 reagent (Invitrogen) and stained for ferritin (red). Scale bar: 5 µM. Image visualization was performed on a LSM 700 (Zeiss) laser scanning inverted confocal microscope with a Plan-Apochromat X63 /1.4 NA oil DIC objective.

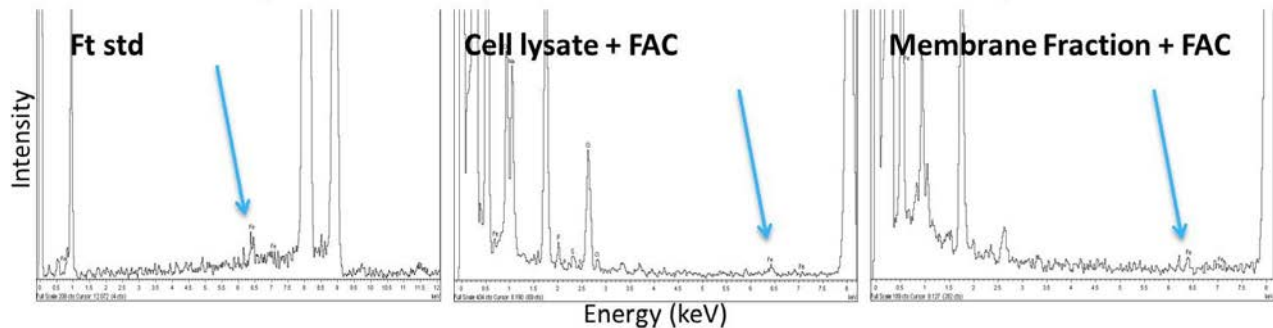


Figure S2. Energy dispersive X-ray spectra of ferritin standard, total cell lysate and membrane-bound vesicles-fractions confirming the presence of iron (peak at 6.4 keV) consistent with the electron-dense particles observed by TEM (Figure 2E) typical of ferritin cores. Note: The pronounced Cu signal comes from the grid used to mount the sample.

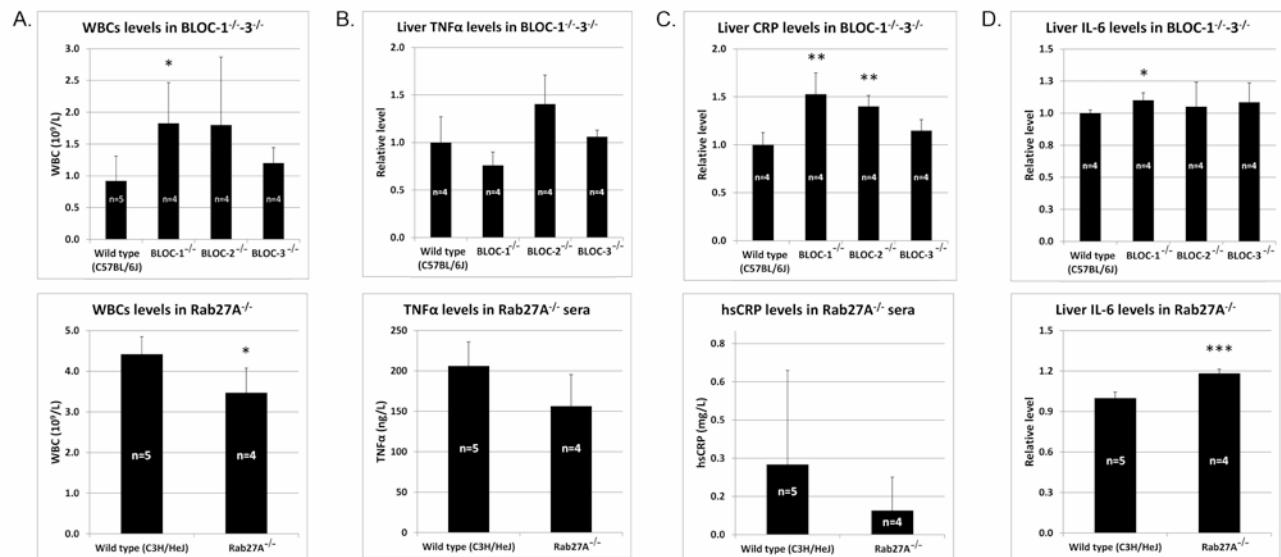


Figure S3. Normal levels of inflammatory markers were observed in mice with trafficking defects of the endo-lysosomal pathways. (A.) White blood cell count (WBC) was determined by a routine veterinary laboratory in a blind manner. Each bar represents mean \pm SD (n=4/5, * p <0.05, ** p <0.01, *** p <0.001). Statistical significance was evaluated by the unpaired t-test by the GraphPad software. (B.) TNF α measurements: Upper panel: Liver lysates were separated on SDS-PAGE (35 μ g protein/lane) and analyzed by Western blot with anti TNF α and actin antibodies. Quantification of protein relative band intensity was evaluated from SDS-PAGE gels (n=4). Lower panel: TNF α measurements in blood were determined by a routine veterinary laboratory. (C.) CRP measurements: Upper panel: Liver CRP was determined by a commercial ELISA kit (Boster, Cat.# EKO977). Lower panel: CRP measurements in blood were determined by a routine veterinary laboratory. (D.) Liver IL-6 was determined by a commercial ELISA kit (eXCELL Biotech Co. Ltd, Cat.# EM004-48). Several evaluations are statistically significant but seems to have no biological significance.

	E-value	Percentage (%) of ferritin sequences with the motif	
		SP negative	SP positive
1.	4.2e-5663	94	100
2.	1.3e-5757	80	100
3.	1.2e-3288	84	62
4.	4.8e-1713	94	48
5.	2.7e-1633	27	53

Figure S4: Five most conserved motifs in the ferritin sequences of organisms with SP negative ferritins. The ferritin sequences from organisms determined to lack a SP on ferritin were scanned for conserved motifs. The scan of the motifs was performed only on sequences longer than 170 amino acids to homogenize the sequences length. The percentage of SP negative and SP positive sequences having the motif is shown. The e-value is compatible to the preliminary motif search in the SP negative group.

A. Table 2: *In Silico* - predicted changes in binding affinity

Ferritin mutant	Computational $\Delta\Delta G_{\text{bind}}$ (kcal/mol)
R79A	2.77
F81A	1.46
L82A	5.42
Q83A	1.09

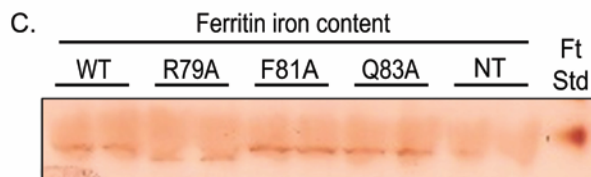
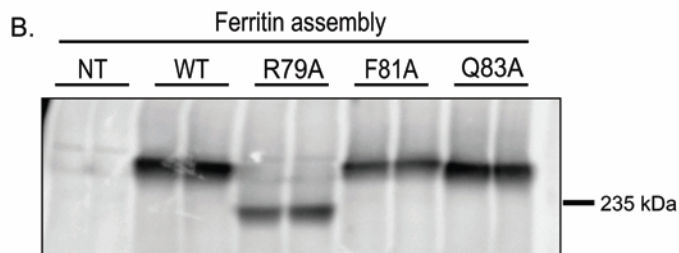


Figure S5: Subunit assembly to a 24-mer and iron content of ferritin with point mutations in the “secretion motif”. (A.) Decrease in binding affinity was predicted *in silico*, using a putative L82A mutation as positive control, as L82 is essential for subunit assembly.³⁴ (B.) HeLa cells with targeted deletions of human ferritin H- and L-subunits (produced by CRISPR/Cas9) were transfected with plasmids coding for wild type (WT) murine H-ferritin or plasmids containing point mutations FTH^{R79A} , FTH^{F81A} or FTH^{Q83A} in the putative secretion motif. After 48 hours cells were lysed and separated by native (non-denaturing) polyacrylamide gel electrophoresis (5% polyacrylamide, 60 $\mu\text{g}/\text{lane}$ protein). Ferritin assembly was visualized by an anti murine H-ferritin antibody. Murine ferritin was absent in non-transfected cells (NT). WT, FTH^{F81A} and FTH^{Q83A} migrated similarly to a ferritin standard lane (standard not shown). FTH^{R79A} migrated slightly faster. (C.) ferritin iron content was determined by Perls Prussian Blue with DAB enhancement staining (200 μg protein/lane). All mutant ferritins contained iron, only the FTH^{R79A} contained slightly less iron than WT and the other two mutations.

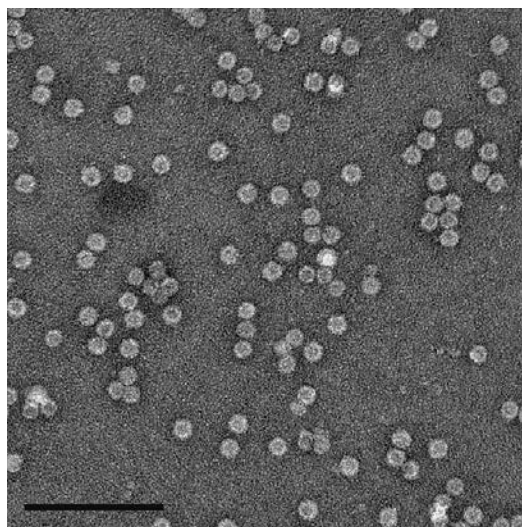


Figure S6. Free ferritin precipitation during the exosome isolation procedure. Standard ferritin was added exogenically to a control medium and purified in parallel to the exosome fractions. For negative staining, samples were re-suspended in 0.1% glutaraldehyde and a drop was mounted on an ion-coated copper grid supported by a carbon-coated film. The grid was stained with 1% uranyl acetate and observed by TEM. Scale bar: 100 nm. The procedure demonstrated, that non-vesicle bound free ferritin is precipitated by the exosome purification protocol.

References

1. Weischenfeldt J, Porse B. Bone Marrow-Derived Macrophages (BMM): Isolation and Applications. *CSH Protoc.* 2008;2008:pdb.prot5080.
2. Huang L, Kuo Y-M, Gitschier J. The pallid gene encodes a novel, syntaxin 13-interacting protein involved in platelet storage pool deficiency. *Nat. Genet.* 1999;23(3):329–332.
3. Li W, Zhang Q, Oiso N, et al. Hermansky-Pudlak syndrome type 7 (HPS-7) results from mutant dysbindin, a member of the biogenesis of lysosome-related organelles complex 1 (BLOC-1). *Nat. Genet.* 2003;35(1):84–89.
4. Zhang Q, Zhao B, Li W, et al. Ru2 and Ru encode mouse orthologs of the genes mutated in human Hermansky-Pudlak syndrome types 5 and 6. *Nat. Genet. N. Y.* 2003;33(2):145–53.
5. Gardner JM, Wildenberg SC, Keiper NM, et al. The mouse pale ear (ep) mutation is the homologue of human Hermansky-Pudlak syndrome. *Proc. Natl. Acad. Sci. U. S. A.* 1997;94(17):9238–9243.
6. Oh J, Bailin T, Fukai K, et al. Positional cloning of a gene for Hermansky-Pudlak syndrome, a disorder of cytoplasmic organelles. *Nat. Genet.* 1996;14(3):300–306.
7. Nguyen T, Wei ML. Hermansky-Pudlak HPS1/pale ear Gene Regulates Epidermal and Dermal Melanocyte Development. *J. Invest. Dermatol.* 2007;127(2):421–428.
8. Wilson SM, Yip R, Swing DA, et al. A mutation in Rab27a causes the vesicle transport defects observed in ashen mice. *Proc. Natl. Acad. Sci. U. S. A.* 2000;97(14):7933–7938.
9. Futter CE, Ramalho JS, Jaissle GB, Seeliger MW, Seabra MC. The Role of Rab27a in the Regulation of Melanosome Distribution within Retinal Pigment Epithelial Cells. *Mol. Biol. Cell.* 2004;15(5):2264–2275.
10. Tolmachova T, Åbrink M, Futter CE, Authi KS, Seabra MC. Rab27b regulates number and secretion of platelet dense granules. *Proc. Natl. Acad. Sci.* 2007;104(14):5872–5877.
11. Dell'Angelica EC. The building BLOC(k)s of lysosomes and related organelles. *Curr. Opin. Cell Biol.* 2004;16(4):458–464.
12. Gautam R, Novak EK, Tan J, et al. Interaction of Hermansky-Pudlak Syndrome Genes in the Regulation of Lysosome-Related Organelles. *Traffic.* 2006;7(7):779–792.
13. Wei A-H, Li W. Hermansky-Pudlak syndrome: pigmentary and non-pigmentary defects and their pathogenesis. *Pigment Cell Melanoma Res.* 2013;26(2):176–192.
14. Li W, Rusiniak ME, Chintala S, et al. Murine Hermansky-Pudlak syndrome genes: regulators of lysosome-related organelles. *BioEssays News Rev. Mol. Cell. Dev. Biol.* 2004;26(6):616–628.
15. Cohen LA, Gutierrez L, Weiss A, et al. Serum ferritin is derived primarily from macrophages through a nonclassical secretory pathway. *Blood.* 2010;116(9):1574–1584.
16. Leichtmann-Bardoogo Y, Cohen LA, Weiss A, et al. Compartmentalization and regulation of iron metabolism proteins protect male germ cells from iron overload. *Am. J. Physiol. Endocrinol. Metab.* 2012;302(12):E1519–1530.
17. McCarthy RC, Kosman DJ. Mechanistic analysis of iron accumulation by endothelial cells of the BBB. *Biometals Int. J. Role Met. Ions Biol. Biochem. Med.* 2012;25(4):665–675.
18. Tong WH, Rouault T. Distinct iron-sulfur cluster assembly complexes exist in the cytosol and mitochondria of human cells. *EMBO J.* 2000;19(21):5692–5700.
19. Brix K, Lemansky P, Herzog V. Evidence for extracellularly acting cathepsins mediating thyroid hormone liberation in thyroid epithelial cells. *Endocrinology.* 1996;137(5):1963–1974.
20. Théry C, Amigorena S, Raposo G, Clayton A. Isolation and characterization of exosomes from cell culture supernatants and biological fluids. *Curr. Protoc. Cell Biol. Editor. Board Juan Bonifacino Al.* 2006;Chapter 3:Unit 3.22.
21. Danino D. Cryo-TEM of soft molecular assemblies. *Curr. Opin. Colloid Interface Sci.* 2012;17(6):316–329.
22. Vaisman B, Santambrogio P, Arosio P, Fibach E, Konijn AM. An ELISA for the H-subunit of human ferritin which employs a combination of rabbit poly- and mice monoclonal antibodies and an enzyme labeled anti-mouse-IgG. *Clin. Chem. Lab. Med.* 1999;37(2):121–125.
23. Meyron-Holtz EG, Ghosh MC, Rouault TA. Mammalian tissue oxygen levels modulate iron-regulatory protein activities in vivo. *Science.* 2004;306:2087–90.

24. UniProt Consortium. UniProt: a hub for protein information. *Nucleic Acids Res.* 2015;43(Database issue):D204-212.
25. Briat J-F. Cellular and whole organism aspects of iron transport and storage in plants. *Mol. Biol. Met. Homeost. Detoxif.* 2005;193-213.
26. Petersen TN, Brunak S, von Heijne G, Nielsen H. SignalP 4.0: discriminating signal peptides from transmembrane regions. *Nat. Methods.* 2011;8(10):785-786.
27. Letunic I, Bork P. Interactive Tree Of Life (iTOL): an online tool for phylogenetic tree display and annotation. *Bioinforma. Oxf. Engl.* 2007;23(1):127-128.
28. Huson DH, Scornavacca C. Dendroscope 3: an interactive tool for rooted phylogenetic trees and networks. *Syst. Biol.* 2012;61(6):1061-1067.
29. Bailey TL, Boden M, Buske FA, et al. MEME SUITE: tools for motif discovery and searching. *Nucleic Acids Res.* 2009;37(Web Server issue):W202-208.
30. Pettersen EF, Goddard TD, Huang CC, et al. UCSF Chimera--a visualization system for exploratory research and analysis. *J. Comput. Chem.* 2004;25(13):1605-1612.
31. Fernandez-Recio J, Totrov M, Skorodumov C, Abagyan R. Optimal docking area: a new method for predicting protein-protein interaction sites. *Proteins.* 2005;58(1):134-143.
32. Heckman KL, Pease LR. Gene splicing and mutagenesis by PCR-driven overlap extension. *Nat. Protoc.* 2007;2(4):924-932.
33. Mancias JD, Wang X, Gygi SP, Harper JW, Kimmelman AC. Quantitative proteomics identifies NCOA4 as the cargo receptor mediating ferritinophagy. *Nature.* 2014;509(7498):105-109.
34. Levi S, Luzzago A, Franceschinelli F, et al. Mutational analysis of the channel and loop sequences of human ferritin H-chain. *Biochem. J.* 1989;264(2):381-388.

